International Journal of High-Rise Buildings
December 2014, Vol 3, No 4, 255-271

International Journal of
High-Rise Buildings
www.ctbuh-korea.org/ijhrb/index.php

Smart System Identification of Super High-Rise Buildings using Limited Vibration Data during the 2011 Tohoku Earthquake

A. Ikeda, Y. Minami, K. Fujita, and I. Takewaki†

Department of Architecture and Architectural Engineering, Kyoto University, Kyoto 615-8540, Japan

Abstract

A method of smart system identification of super high-rise buildings is proposed in which super high-rise buildings are modeled by a shear-bending system. The method is aimed at finding the story shear and bending stiffnesses of a specific story only from the horizontal floor accelerations. The proposed method uses a set of closed-form expressions for the story shear and bending stiffnesses in terms of the limited floor accelerations and utilizes a reduced shear-bending system with the same number of elements as the observation points. A difficulty of prediction of an unstable specific function in a low frequency range can be overcome by introducing an ARX model and discussing its relation with the Taylor series expansion coefficients of a transfer function. It is demonstrated that the shear-bending system can simulate the vibration records with a reasonable accuracy. It is also shown that the vibration records at two super high-rise buildings during the 2011 Tohoku (Japan) earthquake can be simulated with the proposed method including a technique of inserting degrees of freedom between the vibration recording points. Finally it is discussed further that the time-varying identification of fundamental natural period and stiffnesses can be conducted by setting an appropriate duration of evaluation in the batch least-squares method.

Keywords: System identification, Structural health monitoring, Shear-bending model, High-rise building, ARX model, 2011 Tohoku earthquake, Time-varying identification

1. Introduction

The 2011 off the Pacific coast of Tohoku earthquake induced the most intensive vibration of peculiar character in super high-rise buildings in Japan (Tokyo, Nagoya and Osaka) after the construction of such super high-rise buildings. Unfortunately, such vibration characteristics were not taken into account in the design stage of super high-rise buildings up until recently. This earthquake is also thought to be the largest one after the 1923 Great Kanto earthquake (Takewaki et al., 2011a; Kasai et al., 2012; Hisada et al., 2012) which affected the wide area of mega cities in Japan. It seems important to analyze the vibration characteristics of super high-rise buildings for future directions of structural design of super high-rise buildings.

A great deal of interest is focused recently on system identification corresponding to the increasing need for damage detection of building structures under or after earthquakes (Hart and Yao, 1977; Beck and Jennings, 1980; Hoshiya and Saito, 1984; KOzin and Natke, 1986; Agbabian et al., 1991; Koh et al., 1991; Yao and Natke, 1994; Housner et al., 1994; Hjelmstad et al., 1995; Ghanem and Shinozuka, 1995; Shinozuka and Ghanem, 1995; Masri et al., 1996; Doebling et al., 1996; Hjelmstad, 1996; Housner et al., 1997; Kobori et al., 1998; Casciati, 2002; Bernal and Beck, 2004; Lus et al., 2004; Johnson and Smyth, 2006; Nagarajaiah and Basu, 2009; Fujino et al., 2010; Ji et al., 2011; Takewaki et al., 2011b; Abdelrazaq, 2012). Such need of damage detection stems from the accelerated demand of rapid assessment for continuing use of buildings (business continuity planning) after earthquakes. The recognition of actual phenomena and the elucidation of underlying properties are very important for the reliable system identification and damage detection and should be supported by the investigation on actual data and related theories. Filling and narrowing the gap between actual data and the corresponding theories enabled one to accelerate the advancement of the research in this field (Safak, 1995; Celebi, 1996; Beck, 2004; Stewart and Fenves, 1998; Lus et al., 1999; Naeim, 2000; Dunand et al., 2006; Nayeri et al., 2008; Yang and Nagarajaiah, 2012). A comprehensive review of system identification and damage detection has been provided (Kerschen et al., 2006; Nagarajaiah and Basu, 2009; Lee et al., 2010). It is also well-recognized that system identification plays an important role in filling gaps between the constructed structural and infrastructural systems and their structural design models (model refinement) and sophisticating the modeling technique to be able to describe the structural behaviors in a more accurate and reliable manner.

Modal parameter system identification is well-established and a versatile research has been accumulated (for

†Corresponding author: Takewaki I.
Tel: +81-75-383-3294; Fax: +81-75-383-3297
E-mail: takewaki@archi.kyoto-u.ac.jp

example Hart and Yao, 1977; Beck and Jennings, 1980; Safak, 1989; Takewaki et al., 2011b). In the modal parameter system identification, observation at two places is necessary for natural frequency and damping ratio identification. On the other hand, observation at many points is usually required for modal shape identification. It is believed that this often requires a cumbersome task.

In contrast to such modal parameter system identification, the research on physical parameter system identification is scarce and has been developed for direct identification of physical parameters (stiffness and damping coefficients). For example, Takewaki and Nakamura (2000, 2005) introduced a method based on the mathematically eminent work by Udwadia et al. (1978). In that method, a shear building model is used and stiffness and damping coefficients of a specific story are identified directly from the floor accelerations just above and below the specific story. However the method by Takewaki and Nakamura (2000, 2005) has a difficulty resulting from the small signal/noise (SN) ratio in the low frequency range and cannot be applied to high-rise buildings with large aspect ratios (height/width ratio). Independently Hernandez-Garcia et al. (2010a, b) have developed an interesting method of damage detection using a floor-by-floor approach to enhance the efficiency and accuracy of the identification results.

Furthermore a combined method of the modal parameter system identification and the physical parameter system identification is also well used (for example Hjelmstad et al., 1995; Barroso and Rodriguez, 2004). After modal parameters are identified in a stable manner, physical parameters are determined by solving inverse problems.

The number of sensor locations in a building structure is usually limited because of the cost and functionality disturbance problems. The problem of optimal sensor locations and data interpolation is therefore getting much interest recently (Shah and Udwadia, 1978; Udwadia, 1994; Heredia-Zavoni and Esteva, 1998; Worden and Burrows, 2001; Limongelli, 2003; Papadimitriou, 2004; Yi et al., 2011; Limongelli, 2005; Goel, 2008; Yoshitomi et al., 2010; Takewaki et al., 2011b). While a few sensor locations enable the identification of natural periods (lowest few) and the maximum response level of such locations in general, it is desired that more detailed structural properties are identified by constructing even reduced structural models (shear models, shear-bending models, etc).

In this paper, a system identification method for high-rise buildings is explained by introducing a shear-bending model which can describe the overall bending behavior, stemming from column elongation, of such high-rise buildings. While most of the previous methods are based on a shear model and modal identification approaches are often used, a physical-parameter approach, even using a few masses due to the limitation of recording points, is introduced. It is demonstrated that the shear-bending model can simulate the vibration records with a reasonable accuracy. It is shown further that the vibration records at two super high-rise buildings during the 2011 Tohoku (Japan) earthquake can be simulated with the proposed method including a technique of inserting degrees of freedom between the vibration recording points. Inclusion of higher modes in the previous modal approaches seems to have difficulties in the accuracy of identification of higher modes. After an average identification, a further approach for capturing the time-varying mechanical characteristics of a building is proposed.

The above-mentioned difficulty arising in the limit manipulation in the method by Takewaki and Nakamura (2000, 2005) is overcome by introducing an ARX (Auto-Regressive model with eXogenous input) model as in the References (Kuwabara et al., 2012; Maeda et al., 2011). The ARX model is a time-domain model which uses the discrete time step and relates the output data with the input data using the parameters (ARX parameters) and the white noise (see Kuwabara et al., 2012). The weakness of a small SN ratio in the low frequency range in the method (Takewaki and Nakamura, 2000, 2005) is avoided by using the ARX model. Another difficulty due to large aspect ratios is tackled by introducing a shear-bending model introduced in the Reference (Kuwabara et al., 2012). The validity of the method is examined through numerical examples for an assumed building and actual buildings.

Finally it is demonstrated that the time-varying identification of fundamental natural period and story stiffness can be conducted by specifying an appropriate duration of evaluation in the batch least-squares method and an appropriate time of slide for successive identification.

2. Identification Function

2.1. Shear-bending model

Consider an N-story shear-bending building model, as shown in Fig. 1(a), subjected to a horizontal ground acceleration $\ddot{u}_g$. Every story of this shear-bending model consists of an extensional spring and a rotational spring. These two springs are connected in series. Let k_{sj} and k_{bj} denote the stiffness (shear) of the extensional spring and that (bending) of the rotational spring, respectively. Regarding damping, let c_{sj} and c_{bj} denote the damping coefficient of the extensional dashpot and that of the rotational dashpot, respectively. These two dashpots are also connected in series as in springs. The floor mass and its rotational mass moment of inertia are denoted by m_j and J_j, respectively. The story height of the j-th story is given by H_j.

Let **M**, **K** and **C** denote the mass, stiffness and damping matrices of this shear-bending building model and let y_j and θ_j denote the horizontal j-th floor displacement and the angle of j-th floor rotation, respectively. The set of floor displacements and angles of rotation relative to base is denoted by **u**. The equations of motion for this model can be expressed as

$$\mathbf{M}\ddot{\mathbf{u}}+\mathbf{C}\dot{\mathbf{u}}+\mathbf{K}\mathbf{u}=-\mathbf{M}\mathbf{r}\ddot{u}_g \tag{1}$$

where

$$\mathbf{M}=diag(m_1,\ldots,m_N|J_1,\ldots,J_N) \tag{2a}$$

$$\mathbf{C}=\left[\begin{array}{c|c}\mathbf{C}_{HH} & \mathbf{C}_{HR}\\ \hline \mathbf{C}_{HR}^{\ T} & \mathbf{C}_{RR}\end{array}\right] \tag{2b}$$

$$\mathbf{K}=\left[\begin{array}{c|c}\mathbf{K}_{HH} & \mathbf{K}_{HR}\\ \hline \mathbf{K}_{HR}^{\ T} & \mathbf{K}_{RR}\end{array}\right] \tag{2c}$$

$$\mathbf{K}_{HH}=\begin{bmatrix} k_{s1}+k_{s2} & -k_{s2} & \ldots & 0\\ -k_{s2} & \ldots & \ldots & \ldots\\ \ldots & \ldots & k_{sN-1}+k_{sN} & -k_{sN}\\ 0 & \ldots & -k_{sN} & k_{sN}\end{bmatrix} \tag{2d}$$

$$\mathbf{K}_{HR}=\begin{bmatrix} -H_1k_{s1} & H_2k_{s2} & \ldots & 0\\ 0 & \ldots & \ldots & \ldots\\ \ldots & \ldots & \ldots & H_Nk_{sN}\\ 0 & \ldots & 0 & -H_Nk_{sN}\end{bmatrix} \tag{2e}$$

$$\mathbf{K}_{RR}=\begin{bmatrix} H_1^2k_{s1}+k_{b1}+k_{b2} & -k_{b2} & \ldots & 0\\ -k_{b2} & \ldots & \ldots & \ldots\\ \ldots & \ldots & \ldots & -k_{bN}\\ 0 & \ldots & -k_{bN} & H_N^2k_{sN}+k_{bN}\end{bmatrix} \tag{2f}$$

$$\mathbf{u}=\{y_1,\ldots,y_N|\theta_1,\ldots,\theta_N\}^T \tag{2g}$$

$$\mathbf{r}=\{1,\ldots,1|0,\ldots,0\}^T \tag{2h}$$

The sub damping matrices $\mathbf{C}_{HH}$, $\mathbf{C}_{HR}$, $\mathbf{C}_{RR}$ can be derived by replacing k_{si} and k_{bi} with c_{si} and c_{bi} in the sub stiffness matrices $\mathbf{K}_{HH}$, $\mathbf{K}_{HR}$, $\mathbf{K}_{RR}$.

2.2. Equations of motion in frequency domain

Let v_j and ϕ_j denote the shear deformation and the bending deformation, respectively. Then v_j and ϕ_j can be expressed in terms of y_j and θ_j.

$$v_j=y_j-y_{j-1}-\theta_jH_j \tag{3a}$$

$$\phi_j=\theta_j-\theta_{j-1} \tag{3b}$$

Equilibrium of a free body shown in Fig. 1(b) leads to

$$k_{sj}v_j+c_{sj}\dot{v}_j=\sum_{i=j}^{N}\{-m_i(\ddot{u}_g+\ddot{y}_i)\} \tag{4a}$$

$$k_{bj}\phi_j+c_{bj}\dot{\phi}_j= \tag{4b}$$

$$\sum_{i=j}^{N}\{-m_i(\ddot{u}_g+\ddot{y}_i)(H_i^t-H_{j-1}^t)\}+\sum_{i=j}^{N}(-J_i\ddot{\theta}_i)$$

where $H_i^t=\Sigma_{j=1}^{i}H_j$. Usually the second term in the right-hand side of Eq. (4b) can be neglected compared to the first term. Kuwabara et al. (2012) showed that Fourier transformation of Eqs. (3a), (3b) and (4a), (4b) and arrangement of the resulting equations lead to

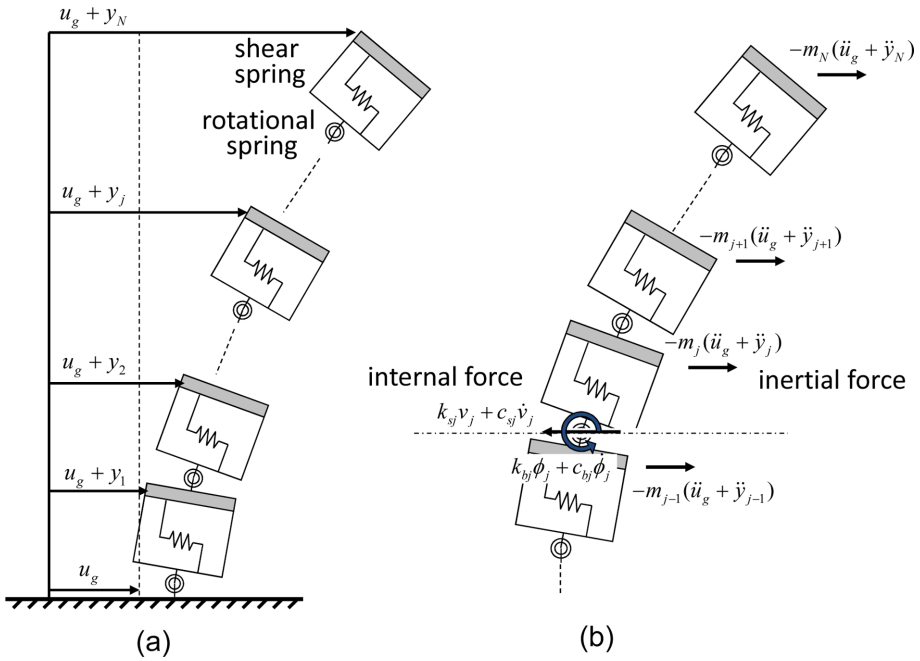


Figure 1. (a) Shear-bending model, (b) Dynamic equilibrium of free body above *j*-th story.

$$\frac{1}{k_{sj}+i\omega c_{sj}}\cdot\frac{\left\{-\omega^2\sum_{i=j}^{N}(-m_i\ddot{Y}_{Ai})\right\}}{(\ddot{Y}_{Aj}-\ddot{Y}_{Aj-1})} \tag{5}$$

$$-\omega^2 H_j\sum_{m=1}^{j}\left[\frac{1}{k_{bm}+i\omega c_{bm}}\frac{\sum_{i=m}^{N}\{-m_i(H_i^t-H_{m-1}^t)\ddot{Y}_{Ai}\}}{(\ddot{Y}_{Aj}-\ddot{Y}_{Aj-1})}\right]=1$$

where $\ddot{Y}_{Ai}=\ddot{U}_g+\ddot{Y}_i$. In Eq. (5), $\ddot{U}_g$, $\ddot{Y}_j$ are Fourier transforms of $\ddot{u}_g$, $\ddot{y}_j$, respectively. Eq. (5) plays a central role in the system identification using the shear-bending model.

The bending and shear stiffnesses have been derived in the Reference (Kuwabara et al., 2012) by introducing the stiffness ratio $R_j = k_{bj} / k_{sj}$.

$$k_{bj}=\frac{R_j+(H_j/M_j)\Sigma_{i=j}^{N}\{m_i(H_i^t-H_{j-1}^t)\}}{\lim_{\omega\to 0}[Re\{F_j(\omega)\}]-(H_j/M_j)\Sigma_{m=1}^{j-1}[\Sigma_{i=m}^{N}\{m_i(H_i^t-H_{m-1}^t)\}/k_{bm}]} \tag{6a}$$

$$k_{sj}=k_{bj}/R_j \tag{6b}$$

where $M_j=\Sigma_{i=j}^{N}m_i$. $F_j(\omega)$ is called 'an identification function' and is defined by

$$F_j(\omega)=\left(\frac{\ddot{U}_{Aj-1}}{\ddot{U}_{Aj}}-1\right)\Big/\left(-\omega^2\sum_{i=j}^{N}m_i\right) \tag{6c}$$

3. Identification Method 1 (Transfer Function Matching)

Introduce the following transfer function (*j*th-story horizontal acceleration to (*j*-1)th-story acceleration) in analogy from shear building models (Takewaki and Nakamura, 2000):

$$G_j=\ddot{U}_{Aj}/\ddot{U}_{Aj-1} \tag{7}$$

Rearrange Eq. (5) using the transfer function, Eq. (7). Application of a new definition $G_G(j)=\Pi_{k=1}^{j}G_k$ to the resulting equation provides the following relation among $G_G(j)(j = 1, \ldots, N)$ (see Minami et al., 2013).

$$\left\{\frac{-\omega^2}{k_{sj}+i\omega c_{sj}}\right\}\sum_{i=j}^{N}\frac{m_iG_G(i)}{G_G(j-1)-G_G(j)} \tag{8}$$

$$-\frac{H_j}{G_G(j-1)-G_G(j)}\sum_{i=1}^{j}\left[\frac{\omega^2}{k_{bi}+i\omega c_{bi}}\sum_{l=i}^{N}\left\{m_lG_G(l)\sum_{k=i}^{l}H_k\right\}\right]=1$$

It can be shown (Minami et al., 2013) that the (*j*-1)th-story transfer function $G_{j\text{-}1}$ can be expressed in terms of the transfer functions from the *j*th through the *N*th story. It should also be noted that $G_{j\text{-}1}$ is a function of $\{R_j\}$. Assume $\{R_j\}$ first and G_N is computed from the records. Then the correspondence between $G_j(\omega, R_j)$ in terms of $\{R_j\}$ and G_j (record) ($j = N$-1, …, 1) is considered. $\{R_j\}$ can be determined by applying the least-squares method (for many frequencies) to $G_{j\text{-}1}$ and the transfer function derived from records by the ARX model. The flowchart of the identi-

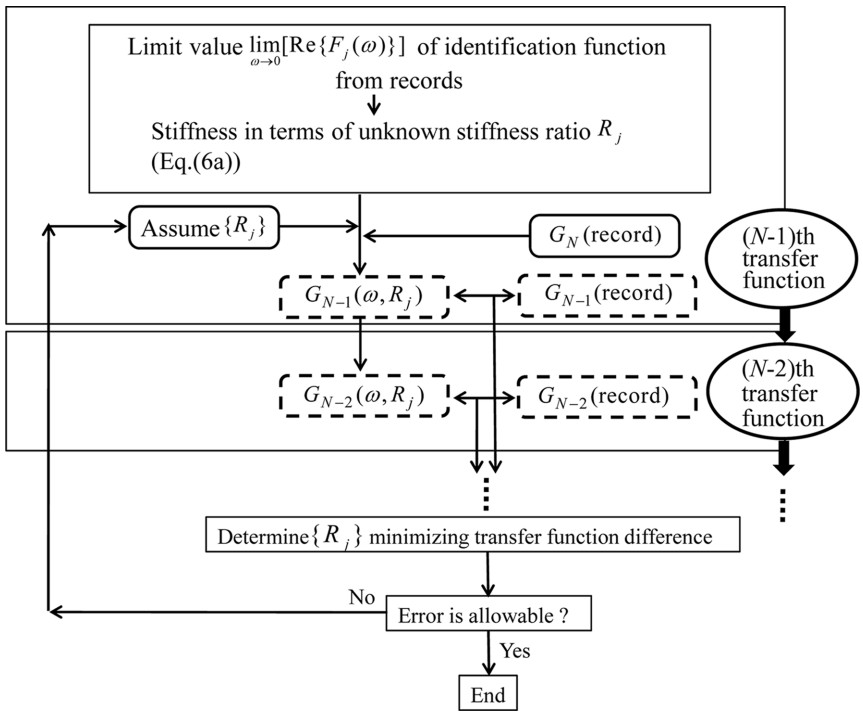


Figure 2. Flowchart of identification method 1.

fication method 1 is shown in Fig. 2.

4. Identification Method 2 (Equilibrium Guarantee)

Consider again the equations of motion, Eq. (1), in time domain for the shear-bending model and the decomposition of the stiffness matrix in Eq. (2c). The static condensation is conducted here. Neglect of the rotational inertia forces and damping forces compared to the stiffness terms provides

$$\mathbf{K}_{HR}{}^{T}\mathbf{y}+\mathbf{K}_{RR}\boldsymbol{\theta}=\mathbf{0} \tag{9}$$

Delete the angle of rotation in the horizontal equilibrium of masses. Then the following relation is derived.

$$\overline{\mathbf{M}}\ddot{\overline{\mathbf{u}}}(t)+\overline{\mathbf{C}}\dot{\overline{\mathbf{u}}}(t)+\overline{\mathbf{K}}\overline{\mathbf{u}}(t)=-\overline{\mathbf{M}}\mathbf{1}\ddot{u}_g(t) \tag{10}$$

where

$$\overline{\mathbf{K}}=\mathbf{K}_{HH}-\mathbf{K}_{HR}\mathbf{K}_{RR}{}^{-1}\mathbf{K}_{HR}{}^{T} \tag{11}$$

$$\overline{\mathbf{C}}=\text{reduced damping matrix} \tag{12}$$

$$\overline{\mathbf{M}}=diag(m_1,\ldots,m_N) \tag{13}$$

$$\overline{\mathbf{u}}(t)=\{y_1,\ldots,y_N\}^{T} \tag{14a}$$

$$\mathbf{1}=\{1,\ldots,1\}^{T} \tag{14b}$$

In the following, a procedure is explained of identification of stiffness matrix components by minimizing un-equilibrium forces in the horizontal direction.

Define the general stiffness and damping matrices by

$$\overline{\mathbf{K}}^{*}=\begin{bmatrix} k_{11}\ldots K_{1N} \\ \ldots\ \ldots\ \ldots \\ k_{N1}\ldots k_{NN} \end{bmatrix} \tag{15a}$$

$$\overline{\mathbf{C}}^{*}=\begin{bmatrix} c_{11}\ldots c_{1N} \\ \ldots\ \ldots\ \ldots \\ c_{N1}\ldots c_{NN} \end{bmatrix} \tag{15b}$$

The equilibrium of the jth floor in the horizontal direction may be expressed by

$$c_{j1}\dot{y}_1+\ldots+c_{jN}\dot{y}_N+k_{j1}y_1+\ldots+k_{jN}y_N=-m_j(\ddot{y}_j+\ddot{u}_g) \tag{16}$$

The process of minimizing the un-equilibrium forces obtained in Eq. (16) by substituting the records $\{y_i\}$, $\{\dot{y}_i\}$, $\{\ddot{y}_i\}$ plays a key role. The minimization conditions can be described by multiplying $\dot{y}_i$ and y_i on Eq. (16) for all masses and all time steps.

$$c_{j1}\dot{y}_1\dot{y}_i+\ldots+c_{jN}\dot{y}_N\dot{y}_i+k_{j1}y_1\dot{y}_i+\ldots+k_{jN}y_N\dot{y}_i=-m_j(\ddot{y}_j+\ddot{u}_g)\dot{y}_i \tag{17}$$

$$c_{j1}\dot{y}_1y_i+\ldots+c_{jN}\dot{y}_Ny_i+k_{j1}y_1y_i+\ldots+k_{jN}y_Ny_i=-m_j(\ddot{y}_j+\ddot{u}_g)y_i \tag{18}$$

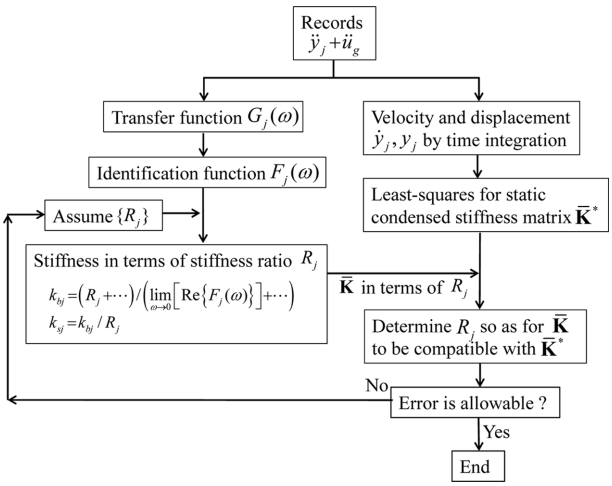


Figure 3. Flowchart of identification method 2.

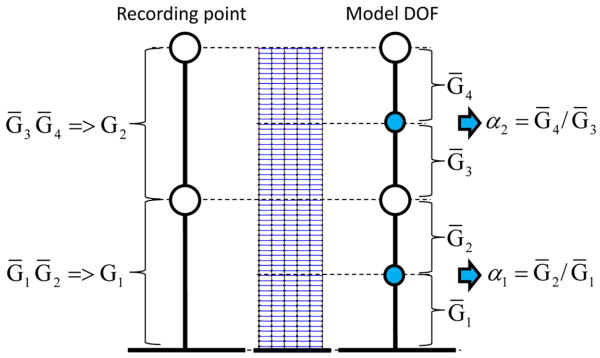


Figure 4. 60-story building frame and recording two points (two additional points are inserted for model DOF).

The detail of identification method 2 can be found in Minami et al. (2013). The flowchart of the identification method 2 is shown in Fig. 3.

5. Insertion of Degrees of Freedom

The number of recording locations is usually very few which causes a difficulty in expressing higher-mode effects in terms of a reduced model with masses at the recording points only. To overcome this difficulty, a technique is introduced such that some degrees of freedom are inserted between these recording points.

Consider an example as shown in Fig. 4. Let $\overline{G}_{2j-1}$, $\overline{G}_{2j}$ denote the transfer functions after the insertion of additional degrees of freedom. It is noteworthy that the following relation holds between $\overline{G}_{2j-1}$, $\overline{G}_{2j}$ and G_j.

$$\overline{G}_{2j-1}\overline{G}_{2j}=G_j \tag{19}$$

Introduce ratios α_j as follows.

$$\lim_{\omega\to 0}\overline{G}_{2j}=\alpha_j\lim_{\omega\to 0}\overline{G}_{2j-1} \tag{20}$$

The newly defined transfer functions can then be expressed in terms of the original transfer function G_j and the ratios α_j.

$$\lim_{\omega\to 0}\overline{G}_{2j-1}=\sqrt{(\lim_{\omega\to 0}G_j)/\alpha_j} \tag{21}$$

$$\lim_{\omega\to 0}\overline{G}_{2j}=\sqrt{\alpha_j(\lim_{\omega\to 0}G_j)} \tag{22}$$

6. Identification of Stiffness using ARX Model

In the previous method (Takewaki and Nakamura, 2000, 2005) for shear building models, the limit manipulation of another identification function $f_j(\omega)=1/F_j(\omega)$ for $\omega\to 0$ is used. However, the identification function often becomes unstable and exhibits a large variability in the low frequency range. To overcome this difficulty, an ARX model is introduced which is a time-domain model. The reliability of the ARX model in this direction has been confirmed in the references (Takewaki and Nakamura, 2009; Maeda et al., 2011). Especially, the applicability of the ARX model to shear building models has been demonstrated in the Reference (Maeda et al., 2011) and the applicability of the ARX model to shear-bending building models has been confirmed in the Reference (Kuwabara et al., 2012). It noted that Maeda et al. (2011) presented the relationships between the ARX parameters and the physical model parameters. This relationship enabled the reliable identification of physical parameters. In this regard, since it is useful to show the essence of the relation between the model stiffness and the ARX parameters, the limited summary of the Reference (Kuwabara et al., 2012) is shown in the following.

The following relation can be derived from the mechanical interpretation, i.e., the j-th floor and (j-1)-th floor move identically at $\omega\to 0$.

$$\lim_{\omega\to 0}Re\{G_j(\omega)\}=1 \tag{23}$$

The following relation also holds because $G_j(\omega)$ should not include linear terms of ω.

$$\lim_{\omega\to 0}\frac{d}{d\omega}\mathrm{Im}\{G_j(\omega)\}=0 \tag{24}$$

Consider the Taylor series expansion of $G_j(\omega)$ as follows.

$$G_j(\omega)=A_0+A_1\omega+A_2\omega^2+\ldots \tag{25}$$

Eq. (23) leads to Eq. (26) and Eq. (24) yields Eq. (27).

$$A_0^R=1 \tag{26}$$

$$A_1^I=0 \tag{27}$$

Since A_0^R and A_1^I are expressed in terms of the ARX parameters (Kuwabara et al., 2012), Eqs. (26) and (27) can be used to enhance the accuracy in the determination of the ARX parameters.

The stiffness can be identified as

$$\lim_{\omega\to 0}\{Re[1/f_j(\omega)]\}=\lim_{\omega\to 0}\{Re[F_j(\omega)]\} \tag{28}$$

$$=\frac{1}{k_{sj}}+(H_j/M_j)\sum_{m=1}^{j}\left[\sum_{i=m}^{N}\{m_i(H_i^t-H_{m-1}^t)\}/k_{bm}\right]=\frac{A_2^R}{M_j}$$

Because A_2^R is also expressed in terms of the ARX parameters (Kuwabara et al., 2012), the stiffness identification problem can be reduced to the estimation problem of the ARX parameters. In other word, once the ARX parameters are obtained, the stiffness can be identified by using Eq. (28) and the assumed stiffness ratio.

It is important to investigate how to determine the number of order of the ARX model. Fig. 5 shows an example of the correspondence of the function 'Fit' with the limit value at zero frequency of the real part of the identification function. The function Fit is defined by

$$\mathrm{Fit}=\left(1-\frac{\sqrt{\sum_{k=1}^{N_d}[\hat{y}(k)-y(k)]^2}}{\sqrt{\sum_{k=1}^{N_d}[y(k)-\bar{y}]^2}}\right)\times 100[\%] \tag{29}$$

where $\hat{y}(k)$ denotes the data expressed by the ARX model and $\bar{y}$ indicates the mean value.

The right ordinate in Fig indicates the limit value at zero frequency of the real part of the identification function.

7. Application to Artificially Simulated Data

In order to validate the proposed identification method, the identification method 2 is applied to simulated data.

Consider a 60-story, 5-span planar steel frame, as shown in Fig. 6, subjected to a ground motion recorded at the first floor of a super high-rise building in Shinjuku, Tokyo during the 2011 Tohoku earthquake. Every span length is

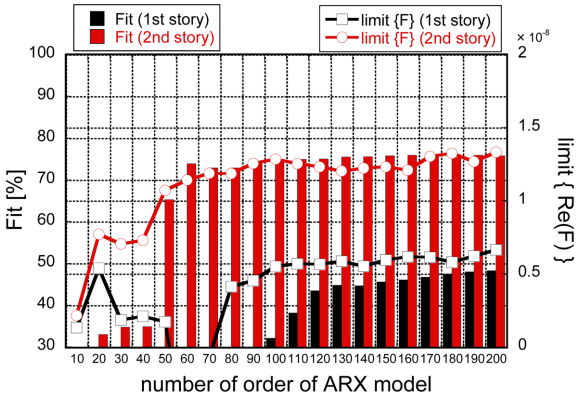


Figure 5. Determination of number of order of ARX model.

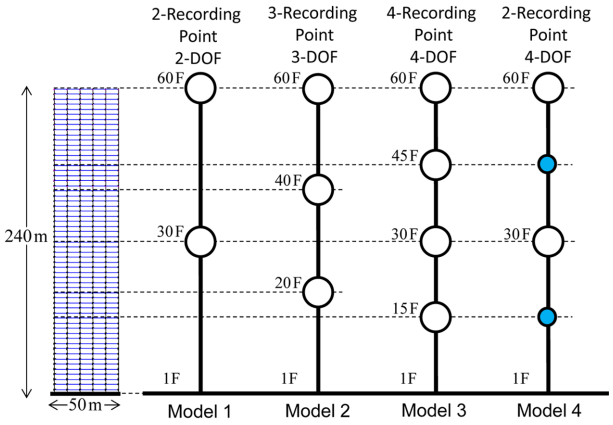


Figure 6. 60-story, 5-span steel building frame and reduced models (Model 1-4).

10(m), every story height is 4(m), every floor mass is 2.56×10^5[kg] and the common member Young's modulus is 2.05×10^5[N/mm^2]. The list of member cross-sections is presented in the Reference (Minami et al., 2013). It is known that this building was retrofitted several years ago using unique viscous oil dampers (avoiding excessive increase of internal force). It was reported that, while the top displacement reached 0.54(m), this building did not experience any visible damage during the 2011 Tohoku earthquake. Elastic time-history response analysis has been conducted using the frame model which can simulate the member behaviors and the obtained responses at representative points were employed as the substitution of recorded data. Model 1 (two points), 2 (three points), 3 (four points) in Fig. 6 have been used as the reduced shear-bending models. The stiffness-proportional damping is employed and the damping ratio is taken as 0.01 in accordance with the frame model. The transfer functions of these models and those of the corresponding shear models are shown in the Reference (Minami et al., 2013) together with those from the Fourier transform of the recorded data without and with the ARX model. The corresponding reduced shear model has been constructed by the procedure similar to the Reference (Takewaki and Nakamura, 2000). The natural periods of lowest few modes of the shear-bending models and the shear models are presented in Tables 1 and 2. The top floor acceleration and displacement are shown in the Reference (Minami et al., 2013). It has been reported that the shear-bending model can simulate the response of the original frame more accurately than the reduced shear model. It has also been confirmed that the shear-bending model with more number of degrees of freedom can represent those of the original models with better accuracy.

Model 4 shown in Fig. 6 is the model with two recording points and two additional points. The method explained in Section 5 has been applied to Model 4. The comparison of the transfer functions has also been made in the Reference (Minami et al., 2013) among the reduced shear-bending and shear models and that from the records. The comparison of the first four natural periods among these models is also shown in Table 3. It has been confirmed that the shear-bending model with more number of degrees of freedom can represent the natural periods with better accuracy. The comparison of the lowest and second eigenmodes among models 1, 3, 4 and frame model can be found in the Reference (Minami et al., 2013). It has been confirmed that models 1, 3 and 4 can represent the eigenmodes up to the second within an acceptable accuracy. The comparison of the top story acceleration and displacement between the frame model (regarded as record) and the reduced models (shear-bending, shear: Model 4) can also be found in the Reference (Minami et al., 2013). It has been concluded that the shear-bending model can simulate the response of the original frame more accurately than the reduced two-mass model (Model 1).

A shear model without reduction is often used in the practical structural design of high-rise buildings. In order to investigate the accuracy of the proposed shear-bending model with few degrees of freedom, the comparison has

Table 1. Natural periods (Model 1, 4)

Mode no.	Original model [s]	Two-mass model (Model 1)		Extended 4-mass model (Model 4)	
		Shear-bending (error [%])	Shear (error)	Shear-bending (error [%])	Shear (error)
1	5.98	6.05 (1.2)	6.21 (3.8)	5.95 (-0.5)	6.00 (0.3)
2	1.98	1.93 (-2.5)	3.17 (60.3)	2.01 (0.5)	2.68 (35.3)
3	1.13			0.77 (-31.8)	2.03 (79.6)
4	0.81			0.68 (-16.0)	1.11 (37.0)

Table 2. Natural periods (Model 2, 3)

Mode no.	Three-mass model (Model 2)		Four-mass model (Model 3)	
	Shear-bending [s] (error [%])	Shear (error)	Shear-bending (error [%])	Shear (error)
1	5.95 (-0.5)	6.04 (1.0)	5.95 (-0.4)	6.02 (0.6)
2	1.99 (0.6)	2.99 (51.0)	1.91 (-3.8)	2.75 (38.9)
3	1.31 (15.6)	1.80 (59.0)	1.42 (25.8)	1.91 (69.4)
4			0.94 (16.5)	1.17 (46.1)

Table 3. Natural periods (60-story shear model)

Mode no.	60-story shear model (error [%])
1	5.97 (0.02)
2	2.34 (18.2)
3	1.48 (31.0)
4	1.08 (33.3)

been made in the Reference (Minami et al., 2013) of the top-story acceleration and displacement among the record, the reduced shear-bending model (Model 3) and the 60-mass shear model without reduction. Table 3 shows the first four natural periods of the 60-mass shear model. I has been reported (Minami et al., 2013) that the reduced shear-bending model (Model 3) can simulate the response of the original frame model more accurately than the 60-mass shear model especially in acceleration.

In order to investigate the usefulness of the proposed identification method and the obtained models, El Centro NS 1940 and Taft EW 1952 have been input to the frame model and the reduced models. The top-story acceleration and displacement have been compared in the Reference (Minami et al., 2013). It can be said that the reduced shear-bending model (Model 3) constructed by the proposed method using a set of vibration records for a specific ground motion can simulate the response (displacement at least) to other ground motions with a reasonable accuracy.

8. Application of Proposed Identification Methods to Actual Buildings

In this section the identification method 1 is applied after the application of the identification method 2. This is because, while the identification method 1 is more accurate than the identification method 2 and sensitive to the initial guess of parameters, the identification method 2 is more robust to the initial guess of parameters. In the identification method 1 used after the application of the identification method 2, the natural periods are determined so that both transfer functions between the measured data and the identification model are compatible.

The most devastating earthquake in Japan after the 1923 Great Kanto earthquake occurred on March 11, 2011. The moment magnitude was 9.0 and this is the largest so far in Japan. The earthquake resulted from the thrust faulting near the subduction zone plate boundary between the Pacific and North America Plates. Nearly 20,000 people were killed or are still missing by that earthquake and the subsequent monster tsunami. Because super high-rise buildings in mega cities in Japan had never been shaken intensively by the so-called long-period ground motions before March 11, 2011, the response of high-rise buildings to such long-period ground motions is one of the most controversial subjects and issues in the field of earthquake-resistant design in Japan.

The proposed identification methods are applied to two actual super high-rise buildings in Japan which were shaken during the 2011 Tohoku earthquake.

8.1. Application to super high-rise building in Osaka bay area

The first actual example is the super high-rise building in Osaka bay area shown in Fig. 7 (Takewaki et al., 2011a, 2012, 2013a; Celebi et al., 2012). This building is a 55-story super high-rise steel building frame (height=256 m: fundamental natural period=5.8 s (long-span direction), 5.3 s (short-span direction)). More detailed data on this building can be found in the reference (Celebi et al., 2012).

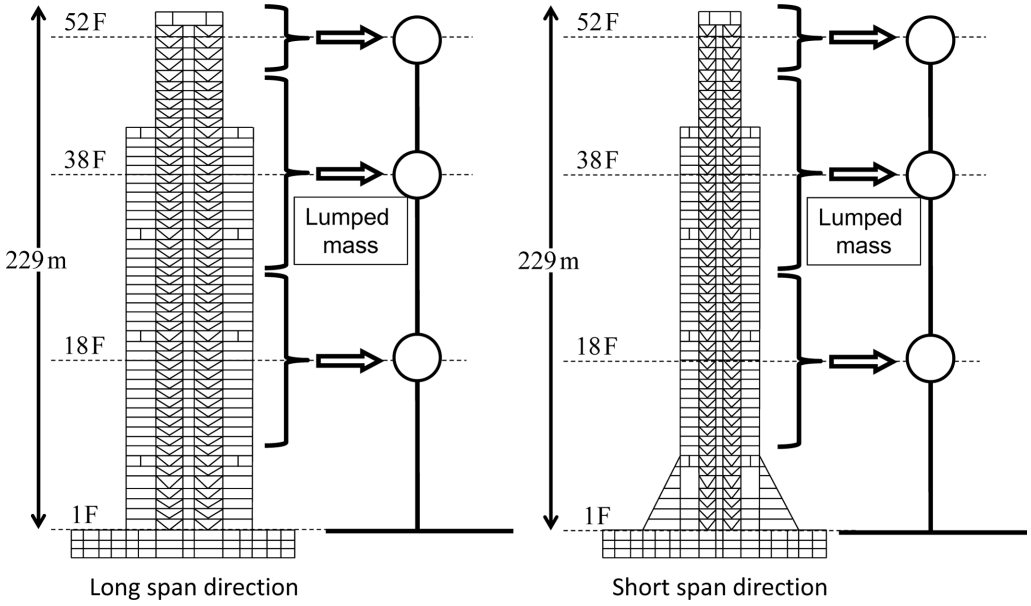


Figure 7. Super high-rise building at Osaka bay area (Minami et al., 2013).

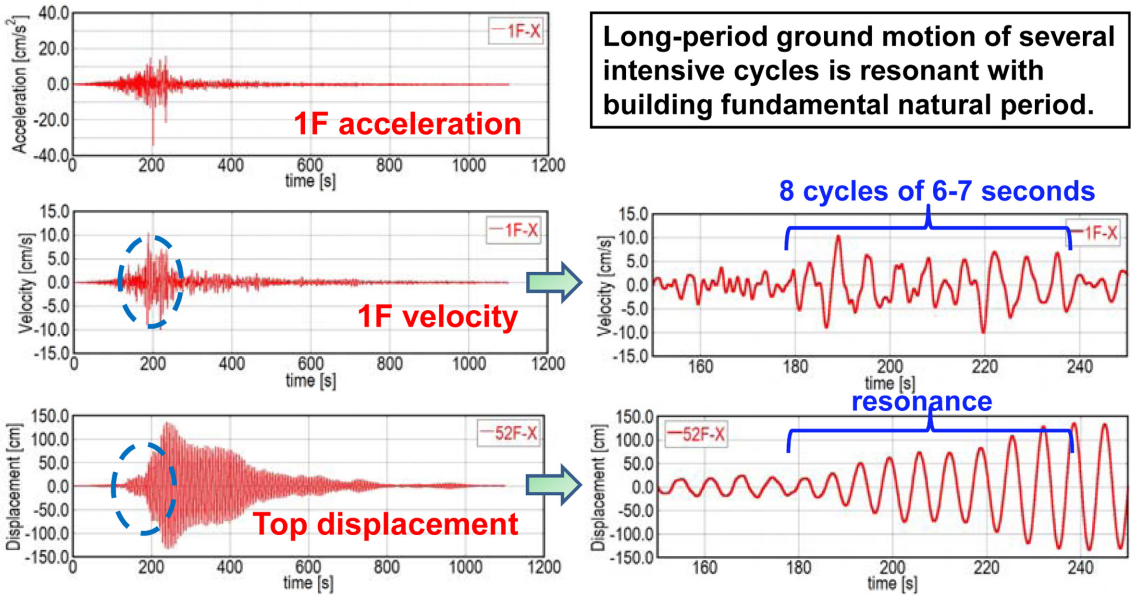


Figure 8(a). Ground acceleration, velocity and top-story displacement (short span direction): Reality of resonance in a 55-story building in Osaka.

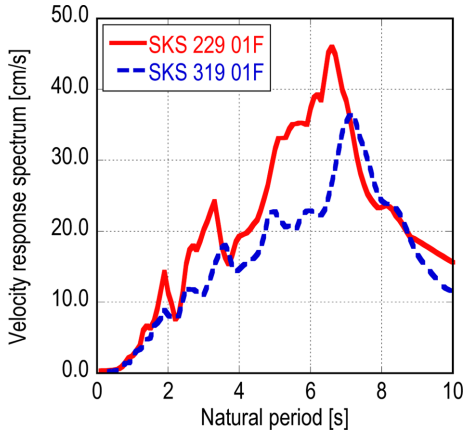


Figure 8(b). Velocity response spectra of ground motion (horizontal two directions, 229: NS, 319: EW).

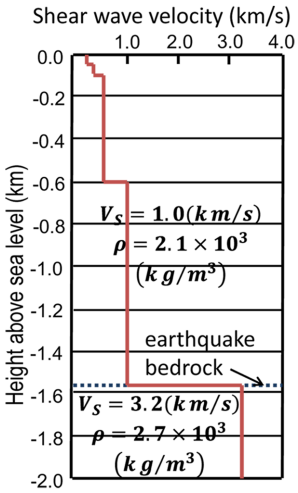


Figure 8(c). Shear wave velocity distribution of surface ground.

It is unusual in Japan that these detailed structural design data are available. This building is reported to have been shaken severely regardless of the fact that Osaka is located far from the epicenter (about 800 km) and the JMA instrumental intensity was 3 in Osaka. It should be pointed out that the level of velocity response spectra of ground motions observed here (first floor) is almost the same as that at the Shinjuku station (K-NET) in Tokyo and the top-story displacement are about 1.4 m (short-span direction) and 0.9 m (long-span direction). Fig. 8(a) shows the response amplification observed in this building during the 2011 Tohoku earthquake. The corresponding velocity response spectra of the ground motion are shown in Fig. 8(b). The direction 229 corresponds to the short-span direction and 319 to the long-span direction. The resonance phenomenon can be explained by using the structure of the surface ground in Fig. 8(c).

Table 4 shows the comparison of natural periods of the original building model (obtained from records) and the reduced shear-bending and shear models in the short-span direction. It can be observed that the shear-bending model can represent the second and third-mode natural periods more accurately than the shear model. Fig. 9 illustrates the top-story accelerations and displacements of the reduced shear-bending and shear models together with the records. In this analysis, the stiffness-proportional damping is used

Table 4. Comparison of modeling accuracy in terms of natural periods (Short span direction)

Mode	Model from records [s]	Shear bending (error [%])	Shear (error [%])
1	6.55	6.64 (1.3)	6.67 (1.9)
2	2.08	2.09 (0.4)	3.26 (56.7)
3	1.11	1.33 (20.1)	1.70 (53.6)

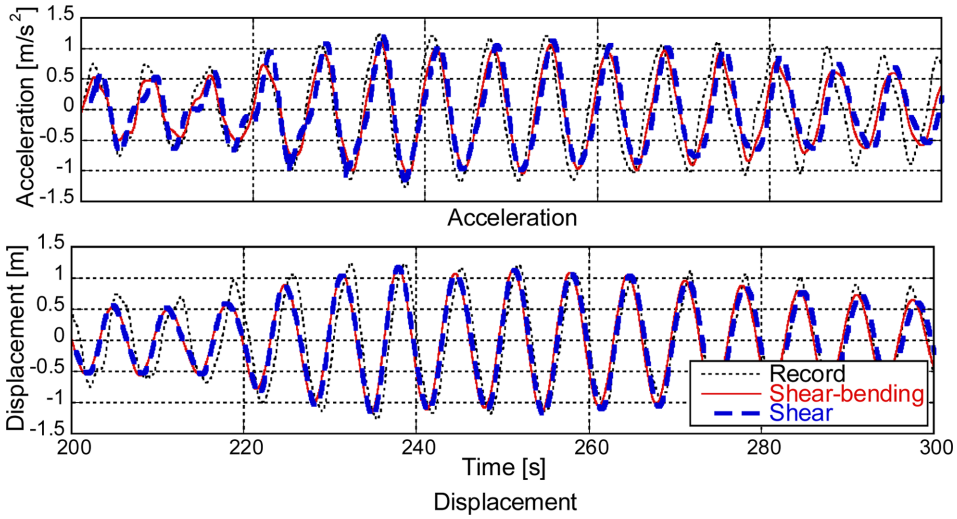


Figure 9. Comparison among record, identified response by shear-bending model and that by shear model (Short span direction).

and the damping ratio is taken as 0.015 judging from the compatibility in transfer functions between the measured data and the identified one. Since this building is just resonant with the surface ground fundamental natural period of about 6.5 s as is well-known, the fundamental-mode vibration component is predominant. For this reason both the reduced shear-bending and shear models can simulate the top-story acceleration and displacement within an acceptable accuracy.

8.2. Application to super high-rise building in Shinjuku, Tokyo

The second actual example is a super high-rise building in Shinjuku, Tokyo as shown in Fig. 10. This building is a 54-story steel building frame (height=223 m: fundamental natural period=6.2 s (short-span direction of 42 m), 5.2 s (long-span direction of 63 m)) retrofitted with nonlinear oil dampers including the supporting bracing system. The nonlinear oil dampers are devised so as to reduce the forces acting on the dampers and surrounding frames. This building experienced the top maximum displacement 0.54(m) during the 2011 Tohoku earthquake. The vibration duration was over 13 minutes. It has also been reported that the building would have attained the top maximum displacement 0.7(m) without the passive dampers.

Table 5 presents the comparison of natural periods of the original building model (obtained from records) and the reduced shear-bending and shear models in the short-span direction. Since the floor mass distribution is not known, an ordinary floor mass of 1.0×10^3 (kg/m^2) is assumed. It can be observed that the shear-bending model can represent the second-mode natural period more accurately than the shear model. Fig. 11(a) presents the recorded acceleration in the short-span direction and Fig. 11(b) shows the comparison of top-story accelerations and displacements in the short-span direction. In this analysis, the stiffness-proportional damping is used and the damping ratio is taken as 0.027 (short-span direction) judging from the compatibility of transfer functions between the measured data and the identified one. It can be found that both the reduced shear-bending and shear models cannot simulate the actual response within an acceptable level. Uncertain factors may be related to (i) the distribution of floor masses, (ii) the structural damping model (stiffness-proportional one was used), (iii) the effect of nonlinear viscous dampers and (iv) restriction of degrees of freedom in the reduced model.

In order to investigate the applicability of the technique explained in Section 5 to this actual building, additional two points (mid-point between the original points) are inserted in the two-mass reduced model (see Fig. 10(b)). The Rayleigh damping model is used and the first and second-mode damping ratios are given as 0.027 and 0.024 in the short-span direction judging from the compatibility of transfer functions between the measured data and the identified one. The comparison has been made in the Re-

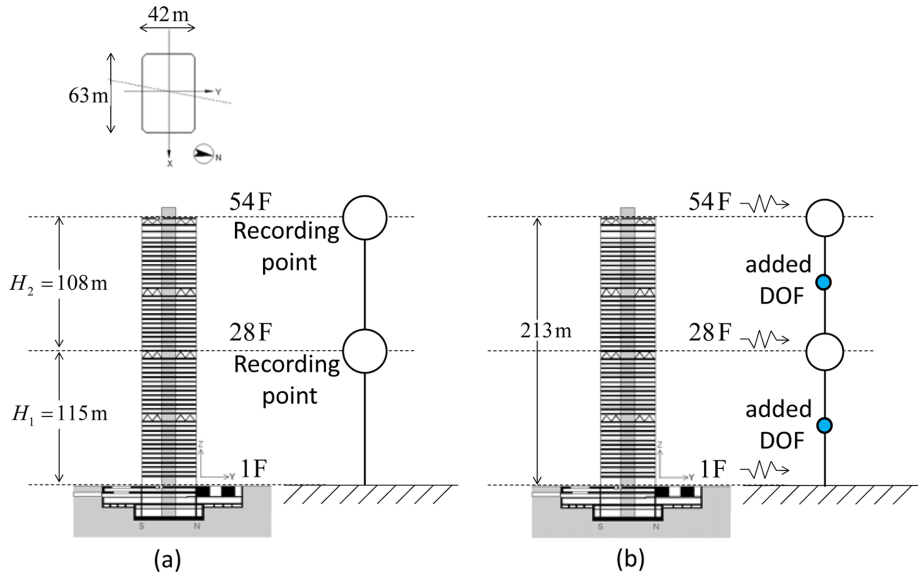


Figure 10. Super high-rise building at Shinjuku, Tokyo (Minami et al., 2013).

Table 5. Comparison of modeling accuracy in terms of natural periods

Mode	Identification from records [s]	Shear bending model (error [%])	Shear model (error [%])
1	6.50	6.64 (2.2)	6.69 (2.9)
2	2.01	2.02 (0.3)	3.05 (51.7)
3	1.04	1.29 (23.6)	2.06 (97.8)
4	-	1.06 (-)	1.49 (-)

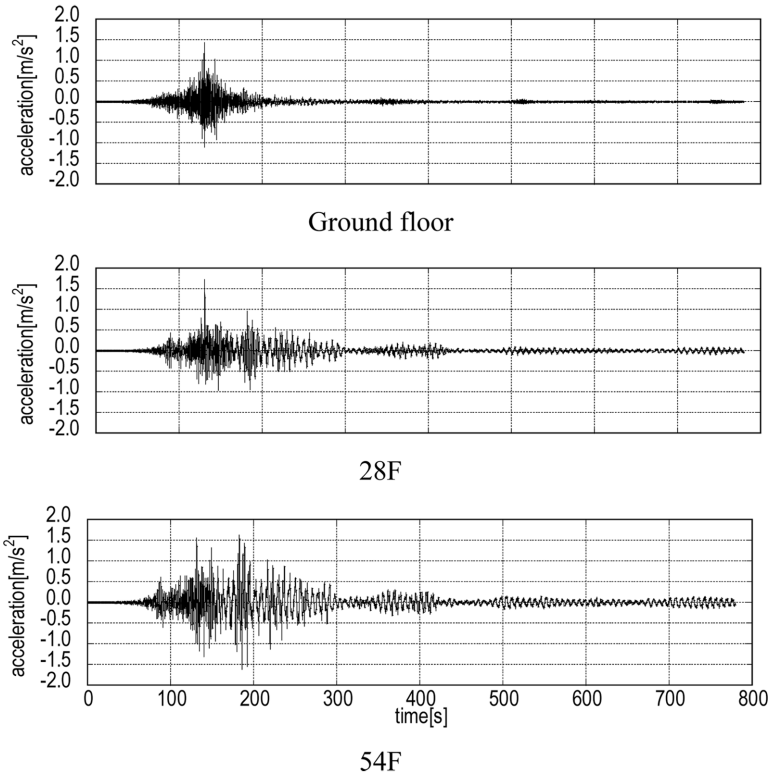


Figure 11(a). Recorded accelerations (short-span direction).

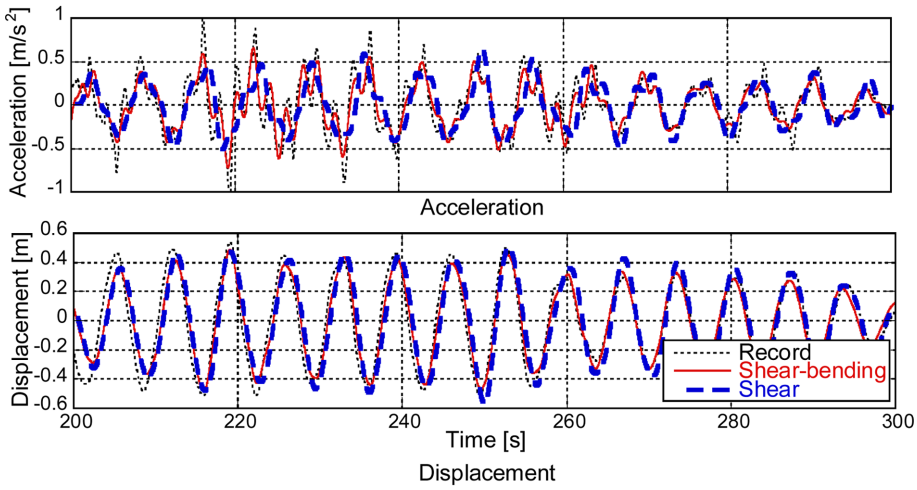


Figure 11(b). Comparison among record in short-span direction, identified response by shear-bending model (model with added degrees of freedom) and that by shear model (model with added degrees of freedom).

ference (Minami et al., 2013) for the natural periods of the original building model (obtained from records) and the reduced shear-bending and shear models. It has been observed that the extended shear-bending model can represent the second and third-mode natural periods more accurately than the shear model. It has also been understood that the extended shear-bending model can represent the higher-mode effect more clearly in acceleration. It has been confirmed that the technique of expansion of degrees explained in Section 5 is promising and reliable.

9. Time-varying Identification

In the previous sections, the batch least-squares method has been used in which the total duration is employed as the duration for estimating a set of ARX parameters. In other words, the averaged values of ARX parameters in the total time duration have been evaluated.

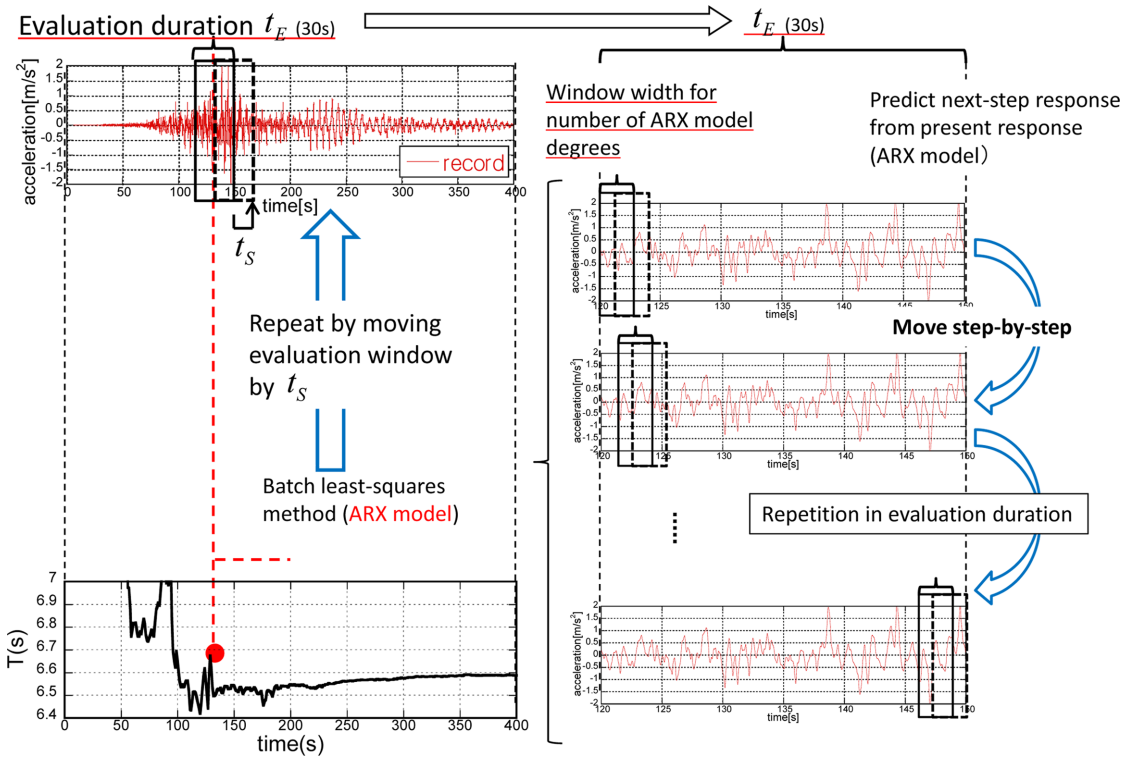


Figure 12. Outline of the proposed time-varying identification.

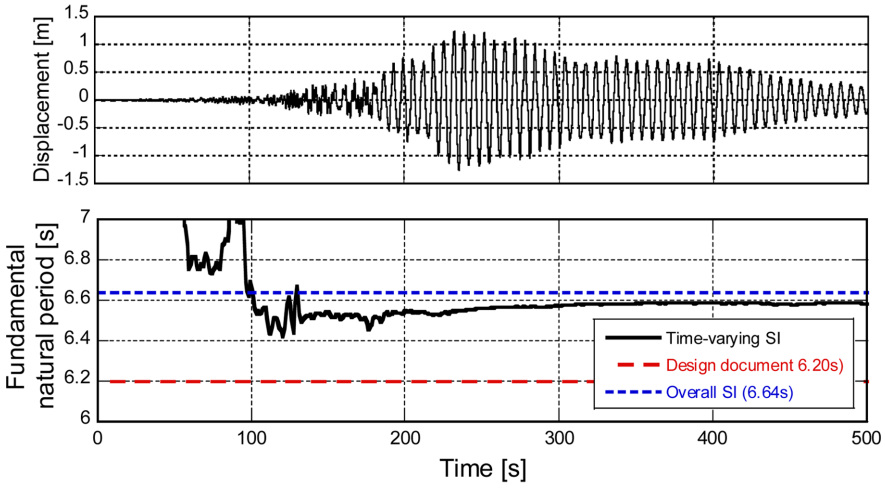


Figure 13. Top-story displacement and fundamental natural period of super high-rise building at Osaka bay area (short-span direction).

It is well known that the natural period of buildings depends on the amplitude of vibration and some portions in the super high-rise building at Osaka bay area (Fig. 7) experienced a limited amount of non-structural damage.

In order to investigate the time-varying mechanical characteristics of a building, a new time-varying identification method is proposed. This method was first proposed by Takewaki and Nakamura (2009) for a shear building model. In this paper, this method is extended to a shear-bending model and stiffnesses are also identified in addition to the natural period.

30 seconds were used as the evaluation time for the batch least-squares method and this process was repeated by moving the window progressively by 1 second later. Fig. 12 presents the outline of the proposed time-varying identification.

Fig. 13 shows the top-story displacement of the super high-rise building at Osaka bay area (Fig. 7) in the short-span direction and the corresponding identified fundamental natural period (Takewaki et al., 2013b). It can be observed that a slight elongation of the fundamental natural period corresponds fairly well with the large displacement amplitude.

Fig. 14 indicates the top-story displacement of the super high-rise building at Shinjuku, Tokyo (Fig. 10) in the short-span direction and the corresponding identified fundamental natural period (Takewaki et al., 2013b). A slight elongation of the fundamental natural period can be seen with the appearance of the large displacement amplitude. As for this building, several data on the fundamental natural period are available and these values are shown in Fig. 14.

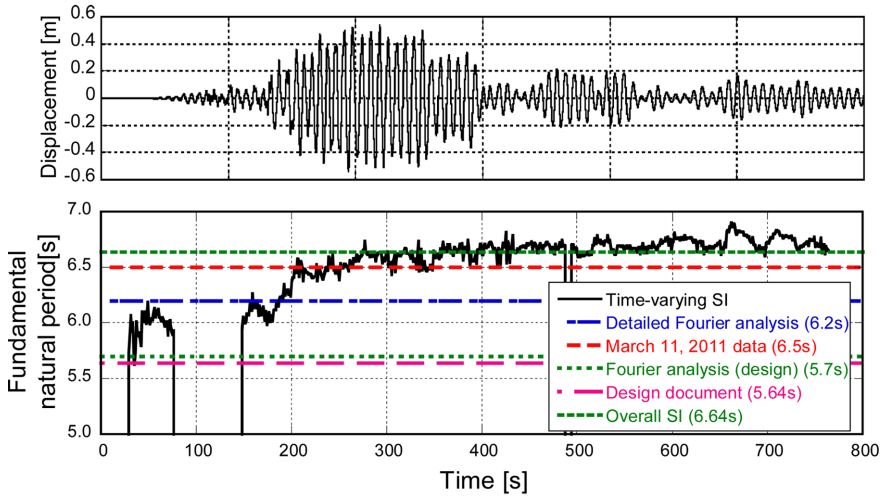


Figure 14. Top-story displacement and fundamental natural period of super high-rise building at Shinjuku, Tokyo (short-span direction).

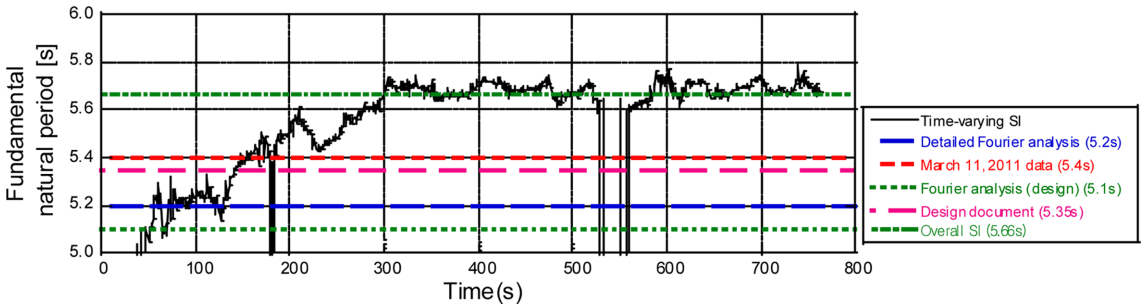


Figure 15. Fundamental natural period of super high-rise building at Shinjuku, Tokyo (long-span direction).

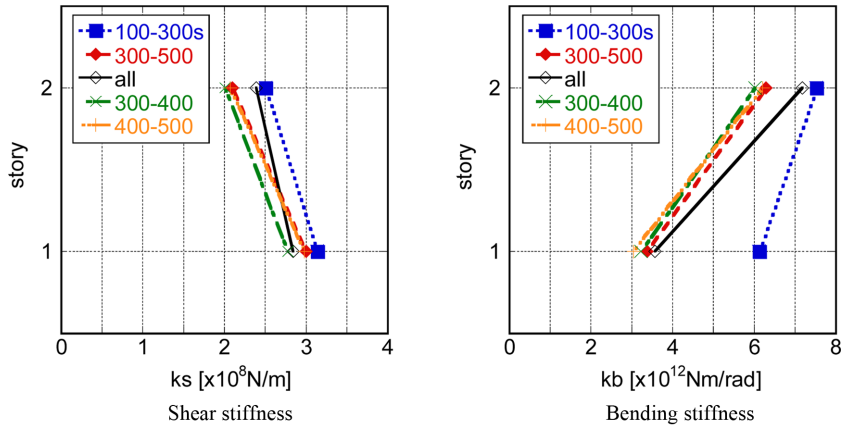


Figure 16. Stiffness change in time in short-span direction.

Fig. 15 shows the identified fundamental natural period in the long-span direction. It can be observed that the fundamental natural period due to the overall system identification result coincides fairly well the transient fundamental natural period after 300 s.

Fig. 16 illustrates the stiffness change in time in the short-span direction. The time windows have been selected as 100~300 s, 300~500 s, 300~400 s, 400~500 s and all (0~800 s). It is observed that the shear and bending stiffnesses can be identified according to the change of the fundamental natural period.

10. Conclusions

A method of smart system identification of super high-rise buildings has been proposed using a shear-bending model. Global and instantaneous identifications have been made feasible. The major accomplishments may be summarized as follows.

(1) The issue in the treatment of shear-bending ratios in a shear-bending model for high-rise buildings (Kuwabara et al., 2012) has been resolved by dealing with such ratios as unknown parameters. Such unknown parameters have been determined so as to fit the transfer functions or minimize un-equilibrium forces acting on floors between the recorded one and the simulated one.

(2) The identification method 1 has been explained which is based on the fitting of the transfer functions between one constructed for the model including unknown shear-bending ratios and the other one constructed directly from the records.

(3) Another identification method has been explained which is based on the minimization of un-equilibrium forces.

(4) A procedure of inserting degrees of freedom between the recording locations seems to be effective for the enhancement of accuracy of the identification methods.

(5) The shear-bending model can simulate higher-mode natural periods of the original model in a more accurate way than the corresponding shear building model.

(6) The ARX model is useful for reliable and accurate identification for the records including noises.

(7) The application to actual data recorded in super high-rise buildings during the 2011 off the Pacific coast of Tohoku earthquake demonstrated that the proposed methods can enhance the reliability and accuracy of identification under noisy environments.

(8) The time-varying identification of modal parameters (fundamental natural period) and physical parameters (stiffness) can be conducted by setting an appropriate du-

ration of evaluation in the batch least-squares method.

Acknowledgements

Part of the present work is supported by the Grant-in-Aid for Scientific Research of Japan Society for the Promotion of Science (No. 21360267, 23656340, 24246095). This support is greatly appreciated. The use of ground motion records from Building Research Institute of Japan, Osaka Prefectural Office and Taisei Co. is also appreciated.

References

Abdelrazaq, A. (2012). Validating the structural behavior and response of Burj Khalifa: Synopsis of the full scale structural health monitoring programs. *Int. J. High-rise Buildings*, 1(1), pp. 37~51.

Agbabian, M. S, Masri, S. F., Miller, R. K., and Caughey, T. K. (1991). System identification approach to detection of structural changes. *J. Engng. Mech.*, *ASCE*, 117(2), pp. 370~390.

Barroso, L. R. and Rodriguez, R. (2004). Damage detection utilizing the damage index method to a benchmark structure. *J. Engng. Mech., ASCE*, 130(2), pp. 142~151.

Beck, J. L. (1996). System identification methods applied to measured seismic response. *Proc. 11th World Conf. Earthq. Eng*., Paper No. 2004.

Beck, J. L. and Jennings, P. C. (1980). Structural identification using linear models and earthquake records. *Earthquake Engng. Struct. Dyn.* 8, pp. 145~160.

Bernal D. and Beck J. (2004). Preface to the Special Issue on Phase I of the IASC- ASCE Structural Health Monitoring Benchmark. *J. Engng. Mech.*, *ASCE*, 130(1), pp. 1~2.

Casciati, F. (ed.) (2002). *Proceedings of* 3*rd World Conference on Structural Control*. John Wiley & Sons: Como.

Celebi, M. (1996). Comparison of damping in buildings under low-amplitude and strong motions. *J. Wing. Eng. & Ind. Appl.* 59(2-3), pp. 309~323.

Celebi, M., Okawa, I., Kashima, T., Koyama, S., and Iiba, M. (2012). Response of a tall building far from the epicenter of the 11 March 2011 M9.0 Great East Japan earthquake and aftershocks. *Struct. Design Tall Spec. Build.* (published online).

Doebling S. W., Farrar C. R., Prime M. B., and Shevitz D. W. (1996) *Damage identification and health monitoring of structural and mechanical systems from changes in their vibration characteristics: A literature review*, Los Alamos National Laboratory Report LA-13070-MS.

Dunand, F., Gueguen, P., Bard, P. Y, Rodgers, J., and Celebi, M. (2006). Comparison of the dynamic parameters extracted from weak, moderate and strong building motion. *Proc. 1st European Conf. of Earthq. Eng. and Seismology*, Geneva, Switzerland, paper 1021.

Fujino, Y., Nishitani, A., and Mita, A. (2010). *Proceedings of* 5*th World Conference on Structural Control and Monitoring, (5WCSCM)*. Tokyo.

Ghanem, R. and Shinozuka, M. (1995). Structural-system identification I: Theory. *J. Engng. Mech., ASCE*, 121(2), pp. 255~264.

Goel, R. K. (2008). Mode-based procedure to interpolate strong motion records of instrumented buildings. *ISET J. Earthquake Technology*, 45(3-4), pp. 97~113.

Hart, G. C. and Yao, J. T. P. (1977). System identification in structural dynamics, *J. Engng. Mech. Div.*, *ASCE*, 103 (EM6), pp. 1089~1104.

Heredia-Zavoni, E. and Esteva, L. (1998). Optimal instrumentation of uncertain structural systems subject to earthquake ground motions. *Earthquake Engng. Struct. Dyn.* 27, pp. 343~362.

Hernandez-Garcia, M. R., Masri, S. F., Ghanem, R., Figueiredo, E., and Farrar, C. R. (2010a). An experimental investigation of change detection in uncertain chain-like systems. *J. Sound Vib.* 329(12), pp. 2395~2409.

Hernandez-Garcia, M., Masri, S. F., Ghanem, R., Figueiredo, E., and Farrar, R. A. (2010b). A structural decomposition approach for detecting, locating, and quantifying nonlinearities in chain-like systems. *Struct. Control Health Monitoring,* 17(7), pp. 761~777.

Hisada, Y., Yamashita, T., Murakami, M., Kubo, T., Shindo, J., Aizawa, K., and Arata, T. (2012). Seismic response and damage of high-rise buildings in Tokyo, Japan, during the Great East Japan earthquake. *Proc. Int. Symp. on Engineering Lessons Learned from the 2011 Great East Japan Earthquake*, March 1-4, 2012, Tokyo, Japan, pp. 1110~1119.

Hjelmstad, K. D, Banan, Mo. R., and Banan, Ma. R. (1995). On building finite element models of structures from modal response. *Earthquake Engng. Struct. Dyn.* 24, pp. 53~67.

Hjelmstad, K. D. (1996). On the uniqueness of modal parameter estimation. *J. Sound and Vib.* 192(2), pp. 581~598.

Hoshiya, M. and Saito, E. (1984). Structural identification by extended Kalman filter. *J. Engng. Mech., ASCE*, 110(12), pp. 1757~1770.

Housner, G. W., Masri, S. F., and Chassiakos, A. G. (eds). (1994). *Proceedings of* 1*st World Conference on Structural Control*. IASC: Los Angeles, CA.

Housner, G., Bergman, L. A., Caughey, T. K., Chassiakos, A. G., Claus, R. O., Masri, S. F., Skelton, R. E., Soong, T. T., Spencer, B. F., and Yao, J. T. P. (1997). Special issue, Structural control: past, present, and future. *J. Engng. Mech.*, *ASCE*, 123(9), pp. 897~971.

Ji, X., Fenves, G. L., Kajiwara, K., and Nakashima, M. (2011). Seismic damage detection of a full-scale shaking table test structure. *J. Struct. Engng. ASCE*, 137(1), pp. 14~21.

Johnson, E. and Smyth, A. (eds). (2006). *Proceedings of* 4*th World Conference on Structural Control and Monitoring, (4WCSCM)*. IASC: San Diego, CA.

Kasai, K., Pu, W., and Wada, A. (2012). Responses of controlled tall buildings in Tokyo subjected to the Great East Japan earthquake, *Proc. Int. Symp. on Engineering Lessons Learned from the 2011 Great East Japan Earthquake*, March 1-4, 2012, Tokyo, Japan, pp. 1099~1109.

Kerschen, G., Worden, K., Vakakis, A. F., and Golinval, J. C. (2006). Past, present and future of nonlinear system identification in structural dynamics, *Mech. Syst. Signal Process.,* 20, pp. 505~592.

Kobori, T., Inoue, Y., Seto, K., Iemura, H., and Nishitani, A. (eds). (1998). *Proceedings of* 2*nd World Conference on*

Structural Control. John Wiley & Sons: Kyoto.

Kozin, F. and Natke, H. G. (1986). System identification techniques. *Struct. Safety* 3, pp. 269~316.

Koh, C. G., See, L. M., and Balendra, T. (1991). Estimation of structural parameters in time domain: a substructure approach. *Earthquake Engng. Struct. Dyn.* 20, pp. 787~801.

Kuwabara, M., Yoshitomi, S., and Takewaki, I. (2012). A new approach to system identification and damage detection of high-rise buildings. *Struct. Control Health Monitoring*, 20(5), pp. 703~727.

Lee, Y. S., Vakakis, A. F., McFarland, D. M., and Bergman, L. A. (2010). A global-local approach to nonlinear system identification: A review, *Struct. Control Health Monitoring,* 17(7), pp. 742~760.

Limongelli, M. P. (2003). Optimal location of sensors for reconstruction of seismic responses through spline function interpolation. *Earthquake Engng. Struct. Dyn.* 32(7), pp. 1055~1074.

Limongelli, M. P. (2005). Performance evaluation of instrumented buildings. *ISET Journal of Earthquake Technology*, 42(2-3), pp. 47~61.

Lus, H., Betti, R., and Longman, R. W. (1999). Identification of linear structural systems using earthquake induced vibration data. *Earthq. Eng. Struct. Dyn.* 28, pp. 1449~1467.

Lus, H., Betti, R., Yu, J., and De Angelis, M. (2004). Investigation of a system identification methodology in the context of the ASCE benchmark problem. *J. Engng. Mech.*, *ASCE*, 130(1), pp. 71~84.

Maeda, T., Yoshitomi, S., and Takewaki, I. (2011). Stiffness-damping identification of buildings using limited earthquake records and ARX model. *J. Struct. Construction Eng.*, Architectural Inst. of Japan; 666, pp. 1415~1423 (in Japanese).

Masri, S. F., Nakamura, M., Chassiakos, A. G., and Caughey, T. K. (1996). A neural network approach to the detection of changes in structural parameters. *J. Engng. Mech.*, *ASCE*, 122(4), pp. 350~360.

Minami, Y., Yoshitomi, S., and Takewaki, I. (2013). System identification of super high-rise buildings using limited vibration data during the 2011 Tohoku (Japan) earthquake. *Structural Control and Health Monitoring*, 20(11), pp. 1317~1338.

Naeim, F. (2000). Learning from structural and nonstructural seismic performance of 20 extensively instrumented buildings. *Proc. 12th World Conf. Earthq. Eng.*, Paper No. 2004.

Nagarajaiah, S. and Basu, B. (2009). Output only modal identification and structural damage detection using time frequency & wavelet techniques. *Earthquake Engng. Engng. Vib*. 8(4), pp. 583~605.

Nayeri, R. D., Masri, S. F., Ghanem, R. G., and Nigbor, R. L. (2008). A novel approach for the structural identification and monitoring of a full-scale 17-story building based on ambient vibration measurements. *Smart Materials and Structures*, 17(2), pp. 1~19.

Papadimitriou, C. (2004). Optimal sensor placement methodology for parametric identification of structural systems. *J. Sound Vib.* 278(4-5), pp. 923~947.

Safak, E. (1995). Detection and identification of soil-structure interaction in buildings from vibration recordings. *J. Struct. Eng. ASCE*, 121(5), pp. 899~906.

Safak, E. (1989). Adaptive modeling, identification, and control of dynamic structural systems. I: Theory, *J. Engng. Mech.*, *ASCE*, 115(11), pp. 2386~2405.

Shah, P. C. and Udwadia, F. E. (1978). A methodology for optimal sensor locations for identification of dynamic systems. *J. Applied Mech., ASME*, 45, pp. 188~196.

Shinozuka, M. and Ghanem, R. (1995). Structural-system identification II: Experimental verification. *J. Engng. Mech., ASCE*, 121(2), pp. 265~273.

Stewart, J. P. and Fenves, G. L. (1998). System identification for evaluating soil-structure interaction effects in buildings from strong motion recordings. *Earthq. Eng. Struct. Dyn.* 27(8), pp. 869~885.

Takewaki, I. and Nakamura, M. (2000). Stiffness-damping simultaneous identification using limited earthquake records. *Earthquake Engng. Struct. Dyn.* 29(8), pp. 1219~1238.

Takewaki, I. and Nakamura, M. (2005). Stiffness-damping simultaneous identification under limited observation. *J. Engng. Mech.*, *ASCE*, 131(10), pp. 1027~1035.

Takewaki, I., Murakami, S., Fujita, K., Yoshitomi, S., and Tsuji, M. (2011a). The 2011 off the Pacific coast of Tohoku earthquake and response of high-rise buildings under long-period ground motions. *Soil Dyn. Earthq. Engrg.* 31 (11), pp. 1511~1528.

Takewaki, I., Nakamura, M., and Yoshitomi, S. (2011b). *System identification for structural health monitoring*, WIT Press (UK).

Takewaki, I. and Nakamura, M. (2009). Temporal variation of modal properties of a base-isolated building during an earthquake. *J. Zhejiang University-SCIENCE A* 11(1), pp. 1~8.

Takewaki, I., Moustafa, A., and Fujita, K. (2012). *Improving the Earthquake Resilience of Buildings: The worst case approach*, Springer (London) (ISBN-10: 1447141431, ISBN-13: 978-1447141433).

Takewaki, I., Fujita, K., and Yoshitomi, S. (2013a). Uncertainties in long-period ground motion and its impact on building structural design: Case study of the 2011 Tohoku (Japan) earthquake. *Engineering Structures*, 49, pp. 119~134.

Takewaki, I., Minami, Y., Ikeda, A., and Fujita, K. (2013b). System identification of super high-rise buildings using limited vibration data during the 2011 Tohoku earthquake. *Proc. of Two Year Memorial Symposium after 2011 Great East Japan Earthquake,* March 27-29, 2013, Tokyo, pp. 313~314.

Udwadia, F. E., Sharma, D. K., and Shah, P. C. (1978). Uniqueness of damping and stiffness distributions in the identification of soil and structural systems. *J. Applied Mech.*, *ASME*, 45, pp. 181~187.

Udwadia, F. E. (1994). Methodology for optimum sensor locations for parameter identification in dynamic systems. *J. Engng. Mech., ASCE*, 120, pp. 368~390.

Worden, K. and Burrows, A. P. (2001). Optimal sensor placement for fault detection. *Engineering Structures* 23(8), pp. 885~901.

Yang, Y. and Nagarajaiah, S. (2012). Time-frequency blind

source separation using independent component analysis for output-only modal identification of highly-damped structures. *J. Struct. Eng. ASCE*, 139(10), pp. 1780~1793.

Yao, J. T. P. and Natke, H. G. (1994). Damage detection and reliability evaluation of existing structures. *Struct. Safety* 15, pp. 3~16.

Yi, T. H., Li, H. N., and Gu, M. (2011). A new method for optimal selection of sensor location on a high-rise building using simplified finite element mode., *Struct. Engng Mech.* 37(6), pp. 671~684.

Yoshitomi, S., Kuwabara, M., Tsuji, M., and Takewaki, I. (2010). Stiffness and damping simultaneous identification based on extrapolation of unrecorded response to ground motion, *Proc. of The First Int Conf. on Advances in Interaction and Multiscale Mechanics (AIMM'10)*, 30 May - 4 June 2010 in Jeju, Korea, pp. 330~349.